

DMD/2018/086132

Catalytic cleavage of disulfide bonds in small molecules and linkers of antibody- drug conjugates

Donglu Zhang*, Aimee Fourie-O'Donohue, Peter S Dragovich, Thomas H Pillow, Jack D
Sadowsky, Katherine R Kozak, Robert T Cass, Liling Liu, Yuzhong Deng, Yichin Liu,
Cornelis ECA Hop, S Cyrus Khojasteh*

Affiliations:

Drug Metabolism & Pharmacokinetics (DZ, RTC, LL, YD, CEAH, SCK), Biochemical
and Cellular Pharmacology (AFO, KRK, YL), Discovery Chemistry (PSD, THP), Protein
Chemistry (JDS), Genentech, Inc., South San Francisco, CA 94080, USA.

Running title: Thioredoxin and glutaredoxin catalyze cleavage of disulfide bonds of linkers of ADC

*Correspondence to: zhang.donglu@gene.com or khojasteh.cyrus@gene.com

Number of text pages=12

Number of tables=1

Number of figures=5

Number of references=36

Number of words in the Abstract= 179

Number of words in the Introduction=670

Number of words in the Discussion=398

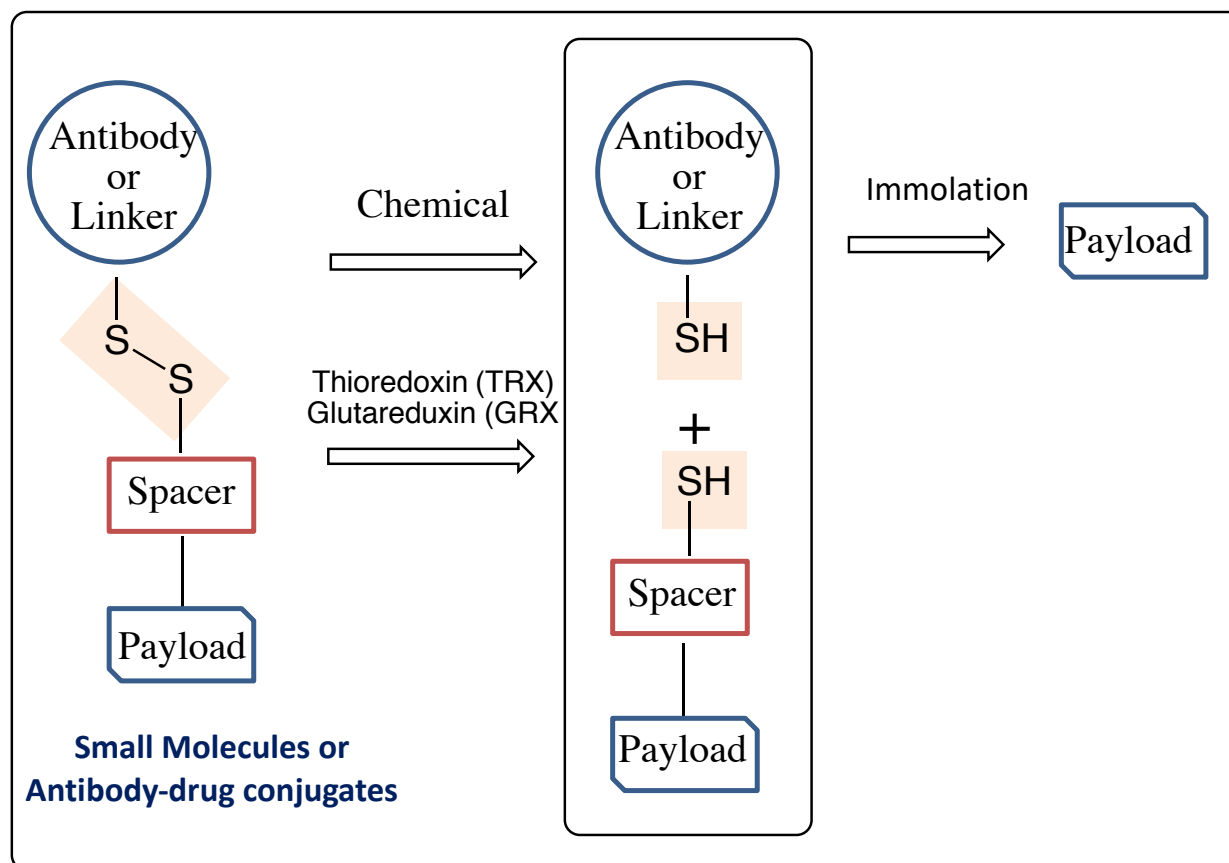
Key Words: ADC linker cleavage, Disulfide linker, Thioredoxin, glutaredoxin

Abbreviations: ADC, antibody drug conjugate; PBD, pyrrolo[2,1-c][1,4]benzodiazepine; GRX, glutaredoxin, GSH, glutathione; TRX, thioredoxin.

Abstract

Catalytic disulfide cleavage is an essential mechanism in cells for protein folding and synthesis; however, the detailed enzymatic mechanism of disulfide bond cleavage in xenobiotics is not well understood. This report describes an enzymatic mechanism of disulfide bond cleavage in xenobiotic small molecules and antibody drug conjugate (ADC) linkers. The chemically stable disulfide bonds in substituted disulfide-containing pyrrolobenzodiazepine (PBD) monomer prodrugs in presence of glutathione or cysteine were found to be unstable in incubations in whole blood of humans and rats. Thioredoxin (TRX) and glutaredoxin (GRX) were the enzymes determined to be involved in this reaction. For a diverse set of drug-linker conjugates, TRX generated cleaved products in the presence of TRX-reductase and NADPH that are consistent with catalytic disulfide cleavage and linker immolation. GRX was less rigorously studied mainly due to availability and lower activity than TRX but its role in the catalytic cleavage was also confirmed for this set of compounds. Collectively, these *in vitro* experiments demonstrate that TRX, as well as GRX, can catalyze the cleavage of disulfide bonds in both small molecules and ADC linkers.

Visual Abstract



Introduction

The disulfide bond (C-S-S-C) is a common structural motif in proteins and has been recently used in targeted drug-delivery approaches (i.e., prodrugs) (Chen and Hu 2009; Vrudhula et al., 2002; Zhang et al., 2017a) that utilize high levels of the reducing agent glutathione (GSH) to selectively release various cytotoxic agents in tumors (Gamcsik et al., 2012; Hatem et al., 2017). Pillow et al. reported a self-immolating disulfide linker (β -mercaptoethyl-carbamate, $-\text{SCH}_2\text{CH}_2\text{OCO}^-$) that can be directly attached to cysteine thiols of antibodies where the cysteine residues are engineered into antibody light or heavy chains (called THIOMABTM antibodies) (Pillow et al., 2017a; Pillow et al., 2017b; Zhang et al., 2016). Cleavage of the disulfide linker was proposed to occur through GSH or cysteine reductive cleavage of the cysteine–thiolate intermediate following conjugate internalization and lysosomal proteolysis. In this mechanism, payload was released after linker immolation following chemical cleavage of the disulfide bond (Pillow et al., 2017a; Pillow et al., 2017b; Zhang et al., 2016). Disulfide bond linkers have also been used in other antibody conjugates (Erickson et al., 2010; Kellogg et al., 2011), chemosensors (Lee et al., 2013), and nanoparticles (Wang et al., 2014; Zhang et al., 2017b).

Pyrrolo[2,1-c][1,4]benzodiazepine (PBD monomer; **1**) and its dimer (PBD dimer; **2**) belong to a class of DNA alkylators that covalently modify DNA minor grooves (Hartley, 2011). Recently, several antibody drug conjugates (ADCs) using PBD analogs as drugs have entered clinical trials (Jeffrey et al., 2013; Saunders et al., 2015). In the process of developing the next generation of ADCs, we sought to design an ADC with a disulfide-containing linker and the prodrug of a cytotoxic payload that could be selectively activated by the high reducing potential present in many intratumor environments following targeted antibody-mediated delivery (Figure 1) (Pei et al., 2018).

Disulfide bonds between cysteines are an integral part of protein structures and are formed during protein synthesis, folding, and post-translational modifications. Thioredoxin (TRX) and glutaredoxin (GRX) are cytosolic enzymes of 10-12 kDa in size that catalyze cleavage of the disulfide bond formed between a cysteine residue and GSH, which is initially formed to protect newly incorporated cysteine residues, or between cysteine residues formed during posttranslational modifications (Azimi et al., 2011; Chen et al.,

2006; Hogg, 2003; Hogg, 2009). TRX can be located outside cells, in the cytoplasm, in the nucleus, or in mitochondria with a cellular concentration of 2-12 μM and a plasma concentration of up to 6 nM. TRX reductase and NADPH are required for TRX catalytic activity (Holmgren and Bjornstedt, 1995; Mustacich and Powis, 2000). GRX concentration in red blood cells can be 1 μM with an optimal pH 8 for catalytic activity. GRX activity also requires a reductase and NADPH or GSH as a cofactor. In this study, the recombinant enzymes TRX and GRX demonstrated catalytic activities for cleavage of disulfide bonds in xenobiotics. The catalytic activities of disulfide cleavage in whole blood are consistent with the activities of TRX and GRX, although low cofactor concentrations in blood may limit their optimal catalytic activities toward xenobiotic disulfides. During the process of testing for disulfide stability in buffer in the presence of GSH or cysteine and whole blood, distinct stability profiles were observed for disulfides with few substitutions at the adjacent carbons. These results suggested that a biological mechanism exists to catalyze certain disulfide cleavages. Subsequently, we conducted experiments to investigate the potential catalytic activity of TRX and GRX, two common oxidoreductase enzymes that are present in whole blood (Pei et al., 2018; Bjornstedt et al., 1995; Butera et al., 2014; Holmgren and Bjornstedt, 1995). Incubation of small molecule disulfide compounds with TRX produced the expected products. Incubation of these enzymes with the disulfide-linker ADC also produced the expected payload **2**. In addition, incubation of an ADC containing both a disulfide prodrug and a disulfide linker produced several products that were consistent with cleavage of either disulfide bond. These results suggested that TRX and GRX can catalyze cleavage of disulfide bonds in small molecules as well as in the linker of an ADC.

Materials and Methods:

Materials

Ammonium formate, formic acid, NADPH, human recombinant human TRX, rat liver TRX reductase, and a proprietary TRX reductase inhibitor (catalog # T9199) were purchased from Sigma-Aldrich (St. Louis, MO, USA). Human GRX I, rat recombinant TRX, and GRX reductase were purchased from Creative Biomart (Shirley, NY). Compounds **1-10** and **12**

were made as described previously (Pei et al., 2018). Synthesis of compounds **11** and **B8** are described in the Supplemental Information section. Human CD22 antibodies with two engineered cysteine residues were generated as described previously (Ohri et al., 2018; Bhakta et al., 2013; Junutula et al., 2016). ADC **13** was synthesized from the linker drug **B8** as described previously (Zhang et al., 2016; Staben et al., 2016). The antibody to drug ratio was 1.9 and 2.0 for ADCs **12** and **13**, respectively.

In vitro incubations in buffer or with enzymes

The compounds were incubated at 10 μ M with 0.03 or 0.2 mM cysteine, or 4 mM GSH, in 100 mM Tris buffer pH 7.0 containing 5% methanol at 37°C. Aliquots were taken at 0, 1, 4, and 24 h and the samples were analyzed by LC-MS/MS.

Selected disulfide prodrugs **3**, **5**, and **10** at 10 μ M and ADCs **12** and **13** at 1.6 μ M (0.25 mg/mL) were separately incubated with human or rat recombinant TRX at 100 nM (1 μ g/mL), with TRX reductase at 20 nM and NADPH (5 mM), or with human recombinant GRX at 100 nM (1.2 μ g/mL) and 80 μ M GSH, all in 100 μ L of Tris buffer (100 mM, pH 7.4) for 1 or 2 h at 37°C in a water bath with shaking at 120 rpm. Control incubations without NADPH or GSH were also included. In addition, the proprietary TRX reductase inhibitor at 1 mM was used in some of incubations. Acetonitrile (0.2 mL) was added to quench the reactions. After centrifugation, aliquots of 10 μ L were injected for LC/MS analysis using the conditions described in next section.

LC/MS analysis for identification of small molecular catabolites

The samples from *in vitro* incubations of buffer, enzymes, or whole blood were injected into a Sciex TripleTOF 5600 with a Hypersil Gold C18 column (100x2.1 mm, 1.9 μ M, Thermo Scientific). The column was eluted at a flow rate of 0.4 mL/min with buffer A (0.1% formic acid in 10 mM ammonium acetate) and buffer B (0.1% formic acid in 10 mM ammonium acetate in 90% acetonitrile) with the following gradient profile: 5% B at 0-0.5 min, 5-25% B at 0.5-8 min, 25-75% B at 8-13 min, 75-95% B at 13-13.5 min, 95% B at 13.5-14.5 min, and 95-5% B at 14.5-15 min. All products were separated and characterized by LC-MS/MS in a positive ESI ion mode. All analytes had the protonated molecular ($[MH]^+$) as the major species with little source fragmentation. Full scan accurate

mass peak areas were used to estimate relative abundance of each species. The disappearance of starting material, estimated on the basis of relative full scan peak areas, was consistent with that estimated based on the relative abundance compared to time 0 h by MS or UV (200-350 nm). The disulfide cleavage versus time profiles were obtained and percent parent remaining at individual time points was reported.

The identification of compounds was performed by LC/MS on a Triple TOF 5600 mass spectrometer (AB Sciex) coupled with HPLC separation. The PBD-dimer (**2**) was identified by a molecular ion at m/z 585.2730 (calculated at 585.2713; $C_{33}H_{37}N_4O_6$) and by major fragments at m/z 504.2144 and 259.1096. Compound **11** was identified by a molecular ion at m/z 781.2968 (calculated at 781.2941; $C_{39}H_{49}N_4O_9S_2$) and by a major fragment at m/z 719.2991. Compound **16** was identified by a molecular ion at m/z 841.2889 (calculated at 841.2788; $C_{40}H_{49}N_4O_{12}S_2$) and by major fragments at m/z 823.2696, 705.2538, 608.2086, and 535.1915. Other compounds were identified by comparison with synthetic materials.

Whole blood stability

Blood of human and rat (100 μ L of pool of mixed gender) was incubated with 10 μ M of each compound (**1-10**) at 37°C for 0, 4, and 24 h ($n = 3$). Acetonitrile (300 μ L) was used to quench the reaction. After vortexing and sonication for 5 min, the samples were centrifuged for 10 min at 2000 xg . The supernatant (50 μ L) was mixed with 200 μ L of water and 10 μ L was analyzed by LC-MS/MS. The GSH analysis was carried out with a Shimadzu Nexera UPLC system coupled to a QTRAP 5500 AB Sciex in positive ion mode. Mobile phase A was water with 0.1% formic acid, and mobile phase B was acetonitrile with 0.1% formic acid. The chromatography was performed on a Thermo HyperCarb column 50x2.1 mm, 3 μ m (Bellefonte PA, USA). Propranolol (100 nM) was used as the internal standard. The calibration curve for quantitation of each compound was constructed by plotting the compound to internal standard peak area ratio versus the nominal concentration of the analyte with a weighted 1/ x quadratic regression.

In preparation for the incubation of ADCs in whole blood, the vendor (Bioreclamation, Westbury NY) shipped cold, whole blood overnight, and stability samples were created immediately upon arrival. Initial dilutions of the ADC source material were made in buffer

(1X PBS, pH7.4, 0.5% BSA, 15 ppm ProClin) so that all molecules were at a concentration of 1 mg/mL. This was followed by a 1:10 dilution (36 μ L of 1 mg/mL solution was diluted in 324 μ L blood or buffer) to generate stability samples with a final concentration of 100 μ g/mL. Once mixed, 150 μ L of the whole blood/buffer stability samples was aliquoted into two separate sets of tubes for the two different time points (0 and 24 h). The 0 h samples were placed in a -80°C freezer and the 24 h samples were placed in a 37°C incubator and shaken (~700 rpm). After 24 h, samples were removed from the incubator and stored in a -80°C freezer until affinity-capture LC-MS was performed. The matrices used to generate the samples were mouse (CB17 SCID), rat (Sprague-Dawley), and human. Whole blood stability samples were analyzed by affinity-capture LC-MS with modifications to the method described previously (Xu, et al., 2011). Briefly, streptavidin-coated (SA) magnetic beads (Thermo Fisher Scientific, Waltham, MA) were washed 2x with HBS-EP buffer (GE Healthcare, Sunnyvale, CA), then mixed with either biotinylated extracellular domain of target (e.g., human erb2) or anti-idiotypic antibody for specific capture using a KingFisher Flex (Thermo Fisher Scientific, Waltham, MA) and incubated for 2 h at room temperature with gentle agitation. After the 2 h, the SA-bead/biotin-capture probe complex was washed 2x with HBS-EP buffer, mixed with stability samples that were diluted 1:16 with HBS-EP buffer and then incubated for 2 h at room temperature with gentle agitation. After 2 h, the SA-bead/biotin-capture probe/sample complex was washed 2x with HBS-EP buffer, followed by deglycosylation overnight with PNGase F (New England BioLabs, Ipswich, MA). The SA-bead/biotin-capture probe/sample complex was then washed 2x with HBS-EP buffer, followed by 2x washes of water (Optima H₂O, Fisher Scientific, Pittsburgh, PA) and finally a 1x wash with 10% acetonitrile. The beads were then placed in a solution of 30% acetonitrile and 0.1% formic acid for elution and incubated for 30 min at room temperature with gentle agitation before being collected. The eluted samples were then loaded onto an LC/MS (Synapt G2-S, Waters, Milford, MA) for analysis.

ADC samples (10 μ L) were injected and loaded onto a PepSwift reversed phase monolithic column (500 μ m \times 5 cm) (Thermo Fisher Scientific, Waltham, MA) maintained at 65°C using a Waters Acquity UPLC system at a flow rate of 20 μ L/min with the following gradient: 20% B (100% acetonitrile and 0.1% formic acid; A is 0.1% formic acid in water)

at 0-2 min, 35% B at 2.5 min, 65% B at 5 min, 95% B at 5.5 min, and 5% B at 6 min. The column was directly coupled for online detection with Waters Synapt G2-S Q-TOF mass spectrometry operated in positive ESI mode with an acquisition range of m/z 500 to 5000.

For stability data analysis, deconvolution of the raw spectrum within a selected ADC elution time window was implemented with Waters BiopharmaLynx 1.3.3 software. Drug loss or modifications were identified according to the corresponding mass shifts from the starting ADC material. Peak labeling and the drug-to-antibody ratio (DAR) calculation were performed with a custom Vortex script (Dotmatics, Bishops Stortford, United Kingdom). Drug loss, cleavage, and formation of adducts were identified according to the corresponding mass shifts from the starting ADC material. The relative abundance of each ADC species in the analytical sample was represented by its MS signal intensity. The relative ratios of ADC with different DARs were calculated by dividing the intensity of the specific ADC species with the intensity of the total ADC species. DAR percent was calculated as previously reported (Staben et al., 2016).

Results

The stability of disulfide bonds in substituted disulfide-containing PBD monomer prodrugs (**3-10**) was tested in incubations with GSH and cysteine (Figure 1). Subsequent tests showed that some stable compounds, which had been selected from a glutathione/cysteine reduction assay, were unstable in incubations in whole blood of humans and rats. Compounds **3-6**, all of which contain the disulfide prodrug functionality, were relatively stable in incubations with 4 mM GSH or 30 μ M cysteine up to 24 h at 37°C (Table 1). In incubations of human or rat whole blood, however, these compounds had a low percent remaining of the starting material at the end of the incubation and were, therefore, unstable under these conditions (Table 1 and Figure S1). In addition, more enzymatic cleavage was observed in rat blood than in human blood. Interestingly, disulfide compounds **7-10**, which have more substitutions on the carbon atoms next to the disulfide bond, showed improved stability compared to the less substituted disulfide compounds **3-6** in both GSH/cysteine reduction assays and whole blood incubations. The product from these whole blood incubations was the expected PBD monomer **1**. Figure 2 (pathway A) shows that chemical reduction of the disulfide bond followed by immolation of the β -mercaptoethyl-carbamate linker produced PBD monomer **1**. To better understand the role of free thiols in the degradation of these disulfide compounds in blood, we also determined GSH and cysteine concentrations in whole blood and in blood cells of rats and humans (Table S1). GSH and cysteine concentrations in the plasma of rats and humans were relatively low at single μ M ranges. On the other hand, GSH concentrations in blood cells reached mM ranges, while cysteine concentrations were at low μ M ranges. These results are consistent with literature values (Gamcsik et al., 2012; Hatem et al., 2017; Johnson et al., 2008; Otani et al., 2011; Sato et al., 2005). In these *in vitro* incubations, the concentrations of the reductants were higher than those found in whole blood or blood cells of human or rat, yet they resulted in much less disulfide cleavage.

Figures 3A and 3C show product profiles of ADC **12** from 24 h incubations in whole blood of human and rat. ADC **12**, which contains a disulfide linker, showed relatively good stability with only low levels of deconjugation products (**P-1**) observed in both human and rat blood samples after a 24 h incubation at 37°C.

A probe ADC molecule **13** was designed to contain both a disulfide prodrug functionality and a disulfide linker on PBD dimer **2**. Compared to ADC **12**, which was relatively stable in whole blood incubations (Figures 3A and 3C), the prodrug ADC **13** was not stable in whole blood of human or rat and showed the formation of multiple products. These products resulted from the loss of one or two prodrug functionalities (-196 Da), or the loss of one or two linker drugs (-LD), or a combination of these degrading processes. Figures 3B, D, E, F show the degradation profiles of ADC **13**. Although the antibody-related product profiles look similar between human and rat, the payload-related product profiles are very different (Figure 4). In incubations with human blood, the intramolecular disulfide **16** was the dominant product with payload **2** and prodrug **11** as minor products. In contrast, incubation in rat blood generated all three compounds (**2**, **11**, **16**) as prominent products. Rat blood presumably has a higher level of degradation activity than human blood, leading to a greater extent of cleavage of **16** and a higher concentration of **2**.

Figure 3 shows the degradation pathway of ADC **13** in human and rat blood. In this pathway, cleavage of the linker disulfide bond resulted in formation of intermediate **14**, which can quickly immolate to form **11**. Disulfide cleavage in the prodrug functionality of ADC **13** generated intermediate **15**, which can immolate to form conjugate **12** (which is also labeled as P3 in the chromatograms). Intermediate **15** can also lead to formation of **16** through intramolecular disulfide formation. Immolation of the less substituted β -mercaptoethyl-carbamate linker in **15** might be slower than that of the β -mercaptoisopropyl-carbamate linker in **14** (Zhang et al., 2018), which would allow for sufficient time to form the intramolecular disulfide **16**. Cleavage of the prodrug disulfide bond appeared to be operative in both human and rat blood. Further degradation of **11**, **12**, or **16** released payload **2**. In this context, cleavage of the linker disulfide bond could be a minor pathway in human blood but a major pathway in rat blood. ADC **13** primarily underwent prodrug disulfide bond cleavage in both human and rat blood to form the intramolecular disulfide **16**. The antibody-related product profile also indicated that cleavage of the prodrug disulfide bond lead to loss of a 196 Da species to form P1-P4 (Figures 3B and D).

The disulfide stability data from the PBD monomer model compounds **3-6** and ADC **13** suggest that there may be an enzymatic mechanism in whole blood that causes instability of these otherwise stable disulfides. Figure 2 (pathway B) shows a proposed mechanism for catalysis of disulfide cleavage through linker immolation, leading to the release of PBD monomer **1** or PBD dimer **2**.

There is a good level (nM to μ M) of TRX and GRX in whole blood in human and animals (Pei et al., 2018; Bjornstedt et al., 1995; Butera et al., 2014; Holgren et al., 1995), which may have caused the instability of the disulfide compounds **3-6**. Experiments were, therefore, conducted using recombinant TRX and GRX enzymes in incubations with these disulfide compounds. The results showed that an appreciable level of PBD monomer **1** was produced from compound **3** in the presence of TRX, TRX-reductase, and NADPH; however, GRX did not form any PBD monomer **1** from **3** in the presence of GSH at a concentration (80 μ M) that did not chemically cleave the disulfide bonds (Figure 5A). Surprisingly, GRX formed a similarly low level of PBD monomer **1** from compounds **5** and **10** (Table 2S), which have different disulfide structures from that in compound **3**. These results suggest that GRX has different specificity and perhaps a narrower range of substrate acceptance than does TRX for catalytic cleavage of disulfide bonds.

We next investigated whether the disulfide linker in ADC **12** is subject to catalytic disulfide cleavage by TRX or GRX. Figure 5B (conditions a, b, and c) showed that incubations of ADC **12** with both human and rat TRX produced PBD dimer **2** after 1-2 h incubations. In comparison, a minimal level of PBD dimer **2** formed in incubations of human TRX without NADPH or in the presence of a TRX-reductase inhibitor (Figure 5B, conditions g and h). Incubations of ADC **12** with GRX produced a lower level of PBD dimer **2** (3-4 fold lower than TRX incubations) (Figure 5B, conditions d, e, and f). No PBD dimer **2** was formed in the control incubation in the presence of 80 μ M GSH cofactor without GRX. The TRX-mediated cleavage of the linker disulfide bond, therefore, appeared to be time- and NADPH-dependent and inhibited by a TRX reductase inhibitor (Figure 5B).

Figure 5C shows PBD-related product formation from incubation of ADC **13** with TRX or GRX under various conditions. Payload **2** was the main product from incubations with human and rat TRX (conditions a, b, and c), while prodrug **11** was a prominent metabolite

formed (conditions a, b, c, and d). This activity was not observed when TRX reductase inhibitor was present in the incubation or no NADPH was used (conditions g and h). The intramolecular disulfide **16** was a minor product of both TRX and GRX incubations. PBD dimer **2** was identified following incubations with TRX in the presence of TRX-reductase and NADPH or GRX at a concentration of GSH that did not cause any level of disulfide linker cleavage (Figure 5C). Similar to whole blood incubations, cleavage of the disulfide linker led to formation of proposed intermediate **14** that could quickly immolate to form prodrug **11**. The disulfide in prodrug **11** could be further cleaved to form payload **2**. Alternatively, disulfide cleavage in the prodrug functionality produced intermediate **15** that underwent relatively slow immolation, leading to formation of intramolecular disulfide **16**. Figure 2S shows the antibody-related product profiles of ADC **12** and **13** in the presence of human or rat TRX as well as human GRX. The conjugate was more extensively degraded in the incubation with TRX than in whole blood (Figures 3B and 3D), as evidenced by an antibody product formed from complete linker cleavage that was not observed in whole blood incubations. Either the prodrug disulfide bond or linker disulfide bond in ADC **13** could be cleaved by TRX or GRX to form a mix of products (Figure 5C). GRX showed a low level of catalytic activity for both types of disulfide bonds.

The linker disulfide bond in ADC **12** was also cleaved by TRX, but the extent of cleavage was much less than that for ADC **13** as a significant amount of starting ADC **12** remained in parallel incubations (Figure 2S, conditions b and d). Comparison of the antibody-related product profiles of ADC **12** and ADC **13** in the presence of TRX clearly showed more extensive degradation of ADC **13** than **12** (Figure 2S). Overall, the prodrug disulfide bond is more susceptible to catalytic cleavage by enzymes than is the disulfide linker bond.

Discussion

Incubations of the disulfide-containing prodrugs **3**, **5**, and **10** with recombinant TRX and GRX in the presence of cofactors showed that the catalytic activity of these enzymes is required to cleave the disulfide bonds in these small molecules. Likewise, incubations of ADC **12** showed the importance of the TRX and GRX enzymes in cleavage of the linker disulfide bond. Incubation of ADC **13** further demonstrated that TRX and GRX can

catalyze cleavage of both prodrug and linker disulfide bonds from the same molecule. These data clearly support catalytic disulfide cleavage activities of TRX and GRX. Both antibody product- and PBD product-profiles were qualitatively similar between the reactions of disulfide compounds with TRX or GRX enzymes in whole blood. Immobilization following disulfide cleavage for the disulfide-containing compounds selected in these studies facilitated product analysis and clean assessment of disulfide cleavage. The disulfide linker cleavage in ADC **12** and **13** suggested that the disulfide bonds that connect engineered-in cysteines and payloads are accessible to enzymes. The variable stabilities of the ADC conjugates from the cysteines engineered at different locations on an antibody may suggest different accessibilities of these linker disulfide bonds to TRX or GRX enzymes (Ohri et al., 2018). Neither of these enzymes is expected to cleave inner disulfide bonds such as inter-chain disulfides of an antibody.

Cellular disulfide cleavage has been implied in a number of previous reports of cell incubations (Zhang et al., 2017b; Butera et al., 2014). TRX has been shown to catalyze the allosteric disulfide bonds in proteins (Hogg, 2003; Hogg, 2009). To our knowledge, there is no prior report of experimental data showing catalytic cleavage of disulfide bonds in xenobiotics by a particular enzyme. Disulfide-containing drugs are rare, which may limit investigations into catalytic disulfide cleavage. Romidepsin is a disulfide-containing HDAC inhibitor prodrug, which acts as an anticancer agent to treat cutaneous T-cell lymphoma (Amengual et al., 2018), and it binds to the thiol in the binding pocket of Zn-dependent histone deacetylase upon disulfide cleavage. TRX and GRX could also be involved in the metabolism of thiol-containing drugs such as albitiazolium (Caldarelli et al., 2012).

Collectively, results support that TRX and GRX in whole blood may catalyze degradation of disulfide-containing prodrugs and disulfide-linker ADC conjugates. Through careful product characterization of disulfide-containing molecules, we demonstrated that TRX and GRX catalyze the disulfide bond cleavage in xenobiotics; thus, representing a new function of TRX and GRX.

Acknowledgements

We would like to thank Hans Erickson and Becca Rowntree for discussion and support.
We would also like to thank Ronitte Libedinsky for her editorial contribution.

Authorship Contributions.

Participated in research design: Zhang, Khojasteh.

Conducted experiments: Zhang, Fourie-O'Donohue, Dragovich, Pillow, Sadowsky,
Kozak, Cass, Liu, Deng, Liu.

Contributed new reagents or analytic tools: Zhang, Dragovich, Pillow, Sadowsky.

Performed data analysis: Zhang, Liu, Deng, Liu, Khojasteh.

Wrote or contributed to the writing of the manuscript: Zhang, Fourie-O'Donohue,
Dragovich, Pillow, Sadowsky, Kozak, Cass, Liu, Deng, Liu, Hop, and Khojasteh.

References:

- Amengual JE, Lichtenstein R, Lue J, Sawas A, Deng C, Lichtenstein E, Khan K, Atkins L, Rada A, Kim HA, et al. (2018) A phase 1 study of romidepsin and pralatrexate reveals marked activity in relapsed and refractory T-cell lymphoma. *Blood* 131: 397-407.
- Azimi I, Wong JW, and Hogg PJ (2011) Control of mature protein function by allosteric disulfide bonds. *Antioxid Redox Signal* 14: 113-26.
- Bhakta S, Raab H, and Junutula JR (2013) Engineering THIOMABs for site-specific conjugation of thiol-reactive linkers. *Methods Mol Biol* 1045: 189-203.
- Bjornstedt M, Hamberg M, Kumar S, Xue J, and Holmgren A (1995) Human thioredoxin reductase directly reduces lipid hydroperoxides by NADPH and selenocystine strongly stimulates the reaction via catalytically generated selenols. *J Biol Chem* 270: 11761-4.
- Butera D, Cook KM, Chiu J, Wong JW, and Hogg PJ (2014) Control of blood proteins by functional disulfide bonds. *Blood* 123: 2000-7.
- Caldarelli SA, Hamel M, Duckert JF, Ouattara M, Calas M, Maynadier M, Wein S, Perigaud C, Pellet A, Vial HJ, and Peyrottes S (2012) Disulfide prodrugs of albitiazolium (T3/SAR97276): synthesis and biological activities. *J Med Chem* 55: 4619-28.
- Chen VM, and Hogg PJ (2006) Allosteric disulfide bonds in thrombosis and thrombolysis. *J Thromb Haemost* 4: 2533-41.
- Chen Y., and Hu L (2009) Design of anticancer prodrugs for reductive activation. *Med Res Rev* 29, 29-64.
- Erickson HK, Widdison WC, Mayo MF, Whiteman K, Audette C, Wilhelm SD, and Singh R (2010) Tumor delivery and in vivo processing of disulfide-linked and thioether-linked antibody-maytansinoid conjugates. *Bioconjug Chem* 21: 84-92.
- Gamcsik MP, Kasibhatla MS, Teeter SD, and Colvin OM (2012) Glutathione levels in human tumors. *Biomarkers* 17: 671-91.
- Hartley JA (2011) The development of pyrrolobenzodiazepines as antitumour agents. *Expert Opin Investig Drugs* 20: 733-44.
- Hatem E, El Banna N, and Huang ME (2017) Multifaceted Roles of Glutathione and Glutathione-Based Systems in Carcinogenesis and Anticancer Drug Resistance. *Antioxid Redox Signal* 27: 1217-1234.
- Hogg PJ (2003) Disulfide bonds as switches for protein function. *Trends Biochem Sci* 28: 210-4.

- 416 Hogg PJ (2009) Contribution of allosteric disulfide bonds to regulation of hemostasis. *J*
417 *Thromb Haemost* 7 Suppl 1: 13-6.
- 418 Holmgren A, and Bjornstedt M (1995) Thioredoxin and thioredoxin reductase. *Methods*
419 *Enzymol* 252: 199-208.
- 420 Jeffrey SC, Burke PJ, Lyon RP, Meyer DW, Sussman D, Anderson M, Hunter JH, Leiske
421 CI, Miyamoto JB, Nicholas ND, et al. (2013) A potent anti-CD70 antibody-drug conjugate
422 combining a dimeric pyrrolobenzodiazepine drug with site-specific conjugation
423 technology. *Bioconjug Chem* 24: 1256-63.
- 424 Johnson JM, Strobel FH, Reed M, Pohl J, and Jones DP (2008) A rapid LC-FTMS method
425 for the analysis of cysteine, cystine and cysteine/cystine steady-state redox potential in
426 human plasma. *Clin Chim Acta* 396: 43-8.
- 427 Junutula JR, and Gerber HP (2016) Next-Generation Antibody-Drug Conjugates (ADCs)
428 for Cancer Therapy. *ACS Med Chem Lett* 7: 972-973.
- 429 Kellogg BA, Garrett L, Kovtun Y, Lai KC, Leece B, Miller M, Payne G, Steeves R,
430 Whiteman KR, Widdison W, et al. (2011) Disulfide-linked antibody-maytansinoid
431 conjugates: optimization of in vivo activity by varying the steric hindrance at carbon atoms
432 adjacent to the disulfide linkage. *Bioconjug Chem* 22: 717-27.
- 433 Lee MH, Yang Z, Lim CW, Lee YH, Dongbang S, Kang C, and Kim JS (2013) Disulfide-
434 cleavage-triggered chemosensors and their biological applications. *Chem Rev* 113: 5071-
435 109.
- 436 Mustacich D, and Powis G (2000) Thioredoxin reductase. *Biochem J* 346: 1-8.
- 437 Ohri R, Bhakta S, Fourie-O'Donohue A, Dela Cruz-Chuh J, Tsai SP, Cook R, Wei B, Ng
438 C, Wong AW, Bos AB, et al. (2018) High-Throughput Cysteine Scanning To Identify
439 Stable Antibody Conjugation Sites for Maleimide- and Disulfide-Based Linkers. *Bioconjug*
440 *Chem* 29: 473-485.
- 441 Otani L, Ogawa S, Zhao Z, Nakazawa K, Umehara S, Yoshimura E, Chang SJ, and Kato
442 H (2011) Optimized method for determining free L-cysteine in rat plasma by high-
443 performance liquid chromatography with the 4-aminosulfonyl-7-fluoro-2,1,3-
444 benzoxadiazole conversion reagent. *Biosci Biotechnol Biochem* 75: 2119-24.
- 445 Pei Z, Chen C, Chen J, dela Cruz-Chuh J, Delarosa R, Deng Y, Fourie-O'Donohue A,
446 Figueroa I, Guo J, Jin W, et al. (2018) Exploration of Pyrrolobenzodiazepine (PBD)-
447 Dimers Containing Disulfide-Based Prodrugs as Payloads for Antibody–Drug Conjugates.
448 *Mol Pharmaceutics* 15: 3979–3996.

- 449 Pillow TH, Sadowsky JD, Zhang D, Yu SF, Del Rosario G, Xu K, He J, Bhakta S, Ohri R,
450 Kozak KR, Ha E, Junutula JR, and Flygare JA (2017a) Decoupling stability and release
451 in disulfide bonds with antibody-small molecule conjugates. *Chem Sci* 8: 366-370.
- 452 Pillow TH, Schutten M, Yu SF, Ohri R, Sadowsky J, Poon KA, Solis W, Zhong F, Del
453 Rosario G, Go MAT, et al. (2017b) Modulating Therapeutic Activity and Toxicity of
454 Pyrrolobenzodiazepine Antibody-Drug Conjugates with Self-Immolative Disulfide Linkers.
455 *Mol Cancer Ther* 16: 871-878.
- 456 Sato H, Shiiya A, Kimata M, Maebara K, Tamba M, Sakakura Y, Makino N, Sugiyama F,
457 Yagami K, Moriguchi T, Takahashi S, and Bannai S (2005) Redox imbalance in
458 cystine/glutamate transporter-deficient mice. *J Biol Chem* 280: 37423-9.
- 459 Saunders LR, Bankovich AJ, Anderson WC, Aujay MA, Bheddah S, Black K, Desai R,
460 Escarpe PA, Hampl J, Laysang A, et al. (2015) A DLL3-targeted antibody-drug conjugate
461 eradicates high-grade pulmonary neuroendocrine tumor-initiating cells in vivo. *Sci Transl*
462 *Med* 7: 302ra136.
- 463 Staben LR, Koenig SG, Lehar SM, Vandlen R, Zhang D, Chuh J, Yu SF, Ng C, Guo J,
464 Liu Y, et al. (2016) Targeted drug delivery through the traceless release of tertiary and
465 heteroaryl amines from antibody-drug conjugates. *Nat Chem* 8: 1112-1119.
- 466 Xu K, Liu L, Saad OM, Baudys J, Williams L, Leipold D, Shen B, Raab H, Junutula JR,
467 Kim A, and Kaur S (2011) Characterization of intact antibody-drug conjugates from
468 plasma/serum in vivo by affinity capture capillary liquid chromatography-mass
469 spectrometry. *Anal Biochem* 412, 56-66.
- 470 Vrudhula VM, MacMaster JF, Li Z, Kerr DE, and Senter PD (2002) Reductively activated
471 disulfide prodrugs of paclitaxel. *Bioorg Med Chem Lett* 12: 3591-4.
- 472 Wang Y, Liu D, Zheng Q, Zhao Q, Zhang H, Ma Y, Fallon JK, Fu Q, Haynes MT, Lin G,
473 et al. (2014) Disulfide bond bridge insertion turns hydrophobic anticancer prodrugs into
474 self-assembled nanomedicines. *Nano Lett* 14: 5577-83.
- 475 Zhang D, Pillow TH, Ma Y, Cruz-Chuh JD, Kozak KR, Sadowsky JD, Lewis Phillips GD,
476 Guo J, Darwish M, Fan P, et al. (2016) Linker Immolation Determines Cell Killing Activity
477 of Disulfide-Linked Pyrrolobenzodiazepine Antibody-Drug Conjugates. *ACS Med Chem*
478 *Lett* 7: 988-993.
- 479 Zhang X, Li X, You Q, and Zhang X (2017a) Prodrug strategy for cancer cell-specific
480 targeting: A recent overview. *Eur J Med Chem* 139: 542-563.
- 481 Zhang S, Guan J, Sun M, Zhang D, Zhang H, Sun B, Guo W, Lin B, Wang Y, He Z, Luo
482 C, and Sun J (2017b) Self-delivering prodrug-nanoassemblies fabricated by disulfide

483 bond bridged oleate prodrug of docetaxel for breast cancer therapy. *Drug Deliv* 24: 1460-
484 1469.

485 Zhang D, Yu SF, Khojasteh SC, Ma Y, Pillow TH, Sadowsky JD, Su D, Kozak KR, Xu K,
486 Polson AG, Dragovich PS, and Hop C (2018) Intratumoral Payload Concentration
487 Correlates with the Activity of Antibody-Drug Conjugates. *Mol Cancer Ther* 17: 677-685.

488

489

Figure legends

Figure 1. Chemical structures of the disulfide-containing prodrugs and ADC conjugates in this study.

Figure 2. Chemical (A) and catalytic (B) disulfide cleavage mechanisms for disulfide-containing prodrugs and disulfide linker-containing ADCs.

Figure 3. Degradation product LC-MS profiles of ADC **13** from human and rat blood incubations.

Figure 4. Proposed payload-related product formation pathways of ADC **13** in incubations in human and rat blood.

Figure 5. PBD-related product LC-MS profiles of disulfide **3** (A), ADC **12** (B), and ADC **13** (C) in catalytic reactions by TRX and GRX.

Table 1. Stabilities of disulfide-containing prodrugs in incubations with GSH, cysteine, or human and rat whole blood.

Compound	% Disulfide remaining			
	GSH @4.0 mM ^a	Cysteine @30 μM ^a	Rat whole blood ^b	Human whole blood ^b
3	56	100	0.1	5
4	21	99	0.3	24
5	68	100	5	80
6	44	98	1	45
7	88	100	87	120 ^c
8	100	100	19	120 ^c
9	100	100	100	108 ^c
10	82	99	124 ^c	124 ^c

^aDisulfide cleavage in the presence of the indicated concentration of GSH or cysteine at 24 h. See Supporting Information for additional details.

^bThe disulfide was incubated in whole blood, and aliquots were analyzed at 24 h. Procaine (10 μM) was used as positive control incubation with <3% remaining after 24 h.

^c Higher than expected % remaining was reported. This is more likely due to the bioanalytical variability.

Figure 1.

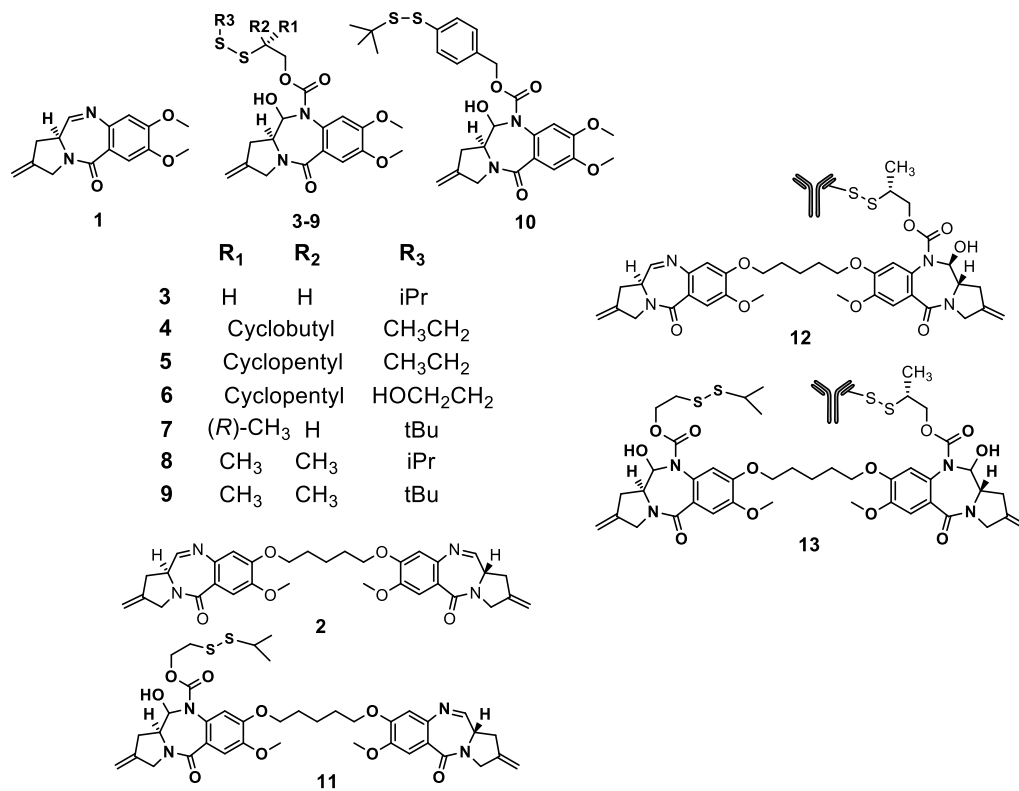


Figure 2.

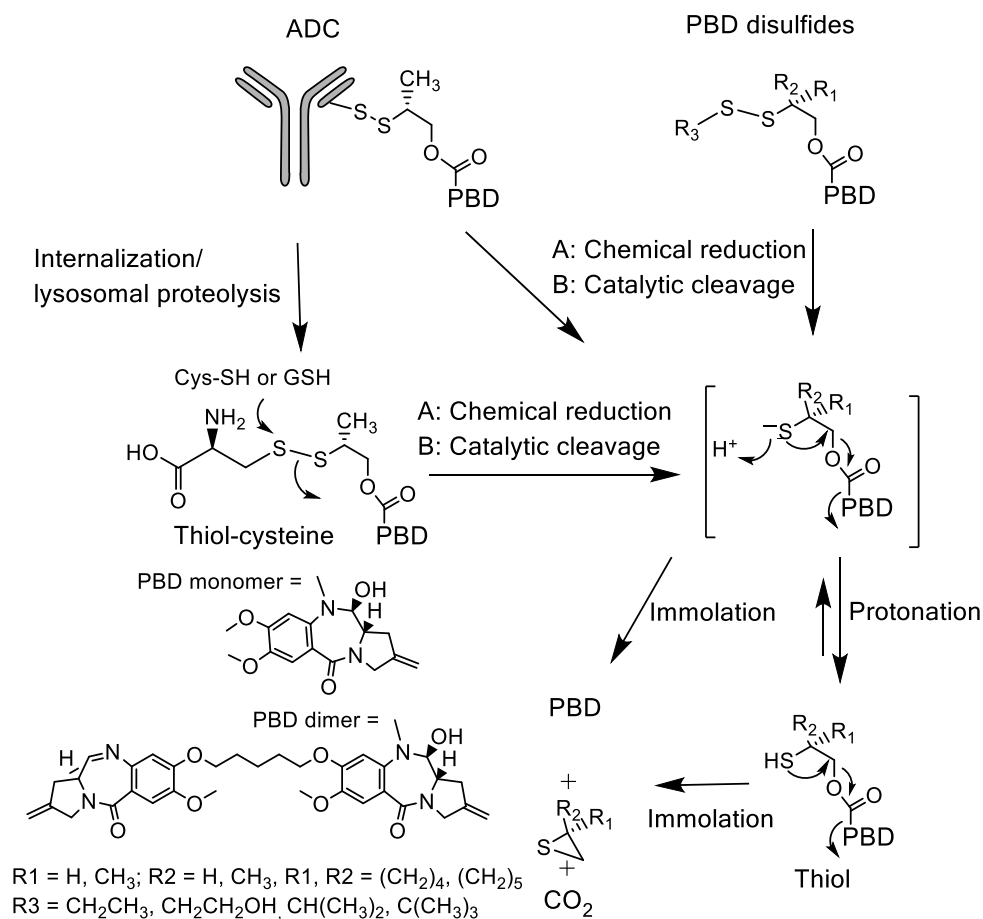


Figure 3.

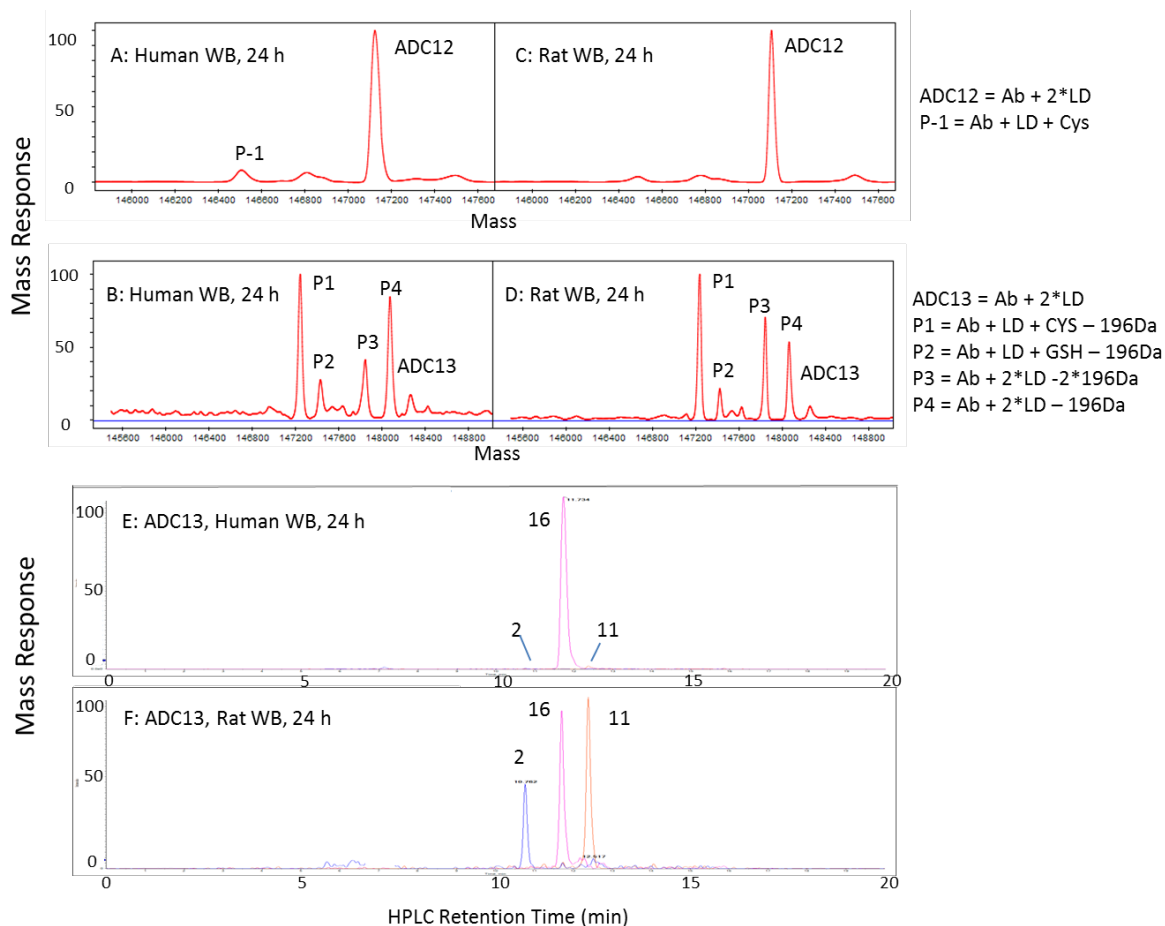


Figure 4.

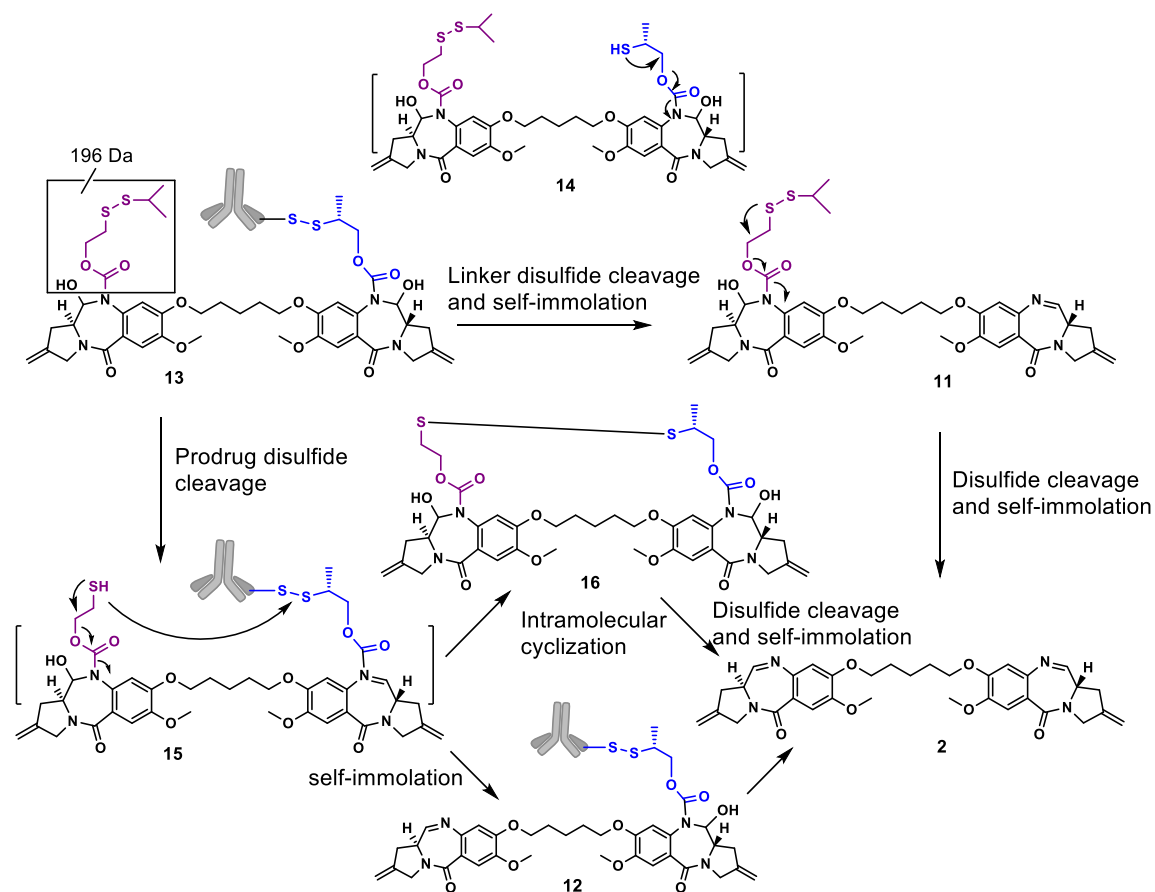
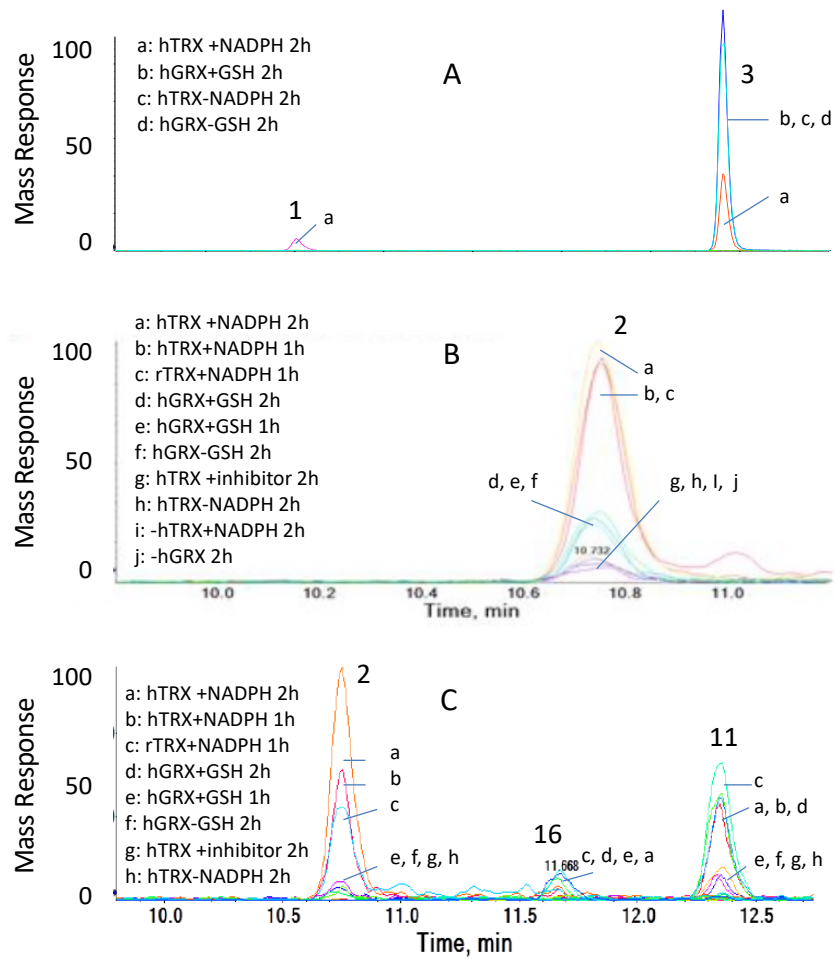


Figure 5.



Supplement Information

Catalytic cleavage of disulfide bonds in small molecules and linkers of antibody-drug conjugates

Donglu Zhang^{1*}, Aimee Fourie-O'Donohue², Peter S Dragovich³, Thomas H Pillow³, Jack D Sadowsky⁴, Katherine R Kozak², Robert T Cass¹, Liling Liu¹, Yuzhong Deng¹, Yichin Liu², Cornelis ECA Hop¹, S Cyrus Khojasteh^{1*}

Affiliations:

Authors Affiliations:

Drug Metabolism & Pharmacokinetics (DZ, RTC, LL, YD, CECAH, SCK), Biochemical and Cellular Pharmacology (AFO, KRK, YL), Discovery Chemistry (PSD, THP), Protein Chemistry (JDS), Genentech, Inc., South San Francisco, CA 94080, USA.

*Correspondence to: zhang.donglu@gene.com

Table 1S. Concentrations of thiol species (GSH, GSSG, cysteine, cysteine) in plasma, blood, and blood cells of human and rat

Table S2. Product formation of disulfide-containing prodrugs and ADC conjugates in incubation with TRX and GRX under various conditions

Figure 1S. Stability of disulfide-containing prodrugs in human and rat blood incubations

Figure 2S. Antibody-related product profiles of ADC **12** and **13** in incubations with TRX and GRX

Synthesis of compounds

Table 1S. Concentrations of thiol species (GSH, GSSG, cysteine, cystine) in plasma, whole blood, and blood cells of human and rat

		GSH (μM)	GSSG (μM)	Cysteine (μM)	Cystine (μM)
Human	Plasma	5.8 ± 0.6	<2.4	<2.4	26.1 ± 3.2
	Blood	284 ± 9	234 ± 25	<2.4	20.6 ± 4.0
	Blood cells	855 ± 50	315 ± 42	<2.4	11.9 ± 5.0
Rat	Plasma	7.8 ± 0.9	13.7 ± 1.1	<2.4	29.8 ± 1.3
	Blood	518 ± 26	92.0 ± 5.9	<2.4	23.7 ± 1.5
	Blood cells	1450 ± 64	160 ± 8	29.4 ± 6.9	12.9 ± 3.0

The samples were treated with 5 volumes of 0.5 N perchloric acid with vortex and sonication for 5 min. The samples were analyzed by LC/MS/MS.

N=4, LLOQ = 1 μM (GSH), 2.4 μM (cysteine), 2.4 μM (GSSG), and 0.4 μM (cystine).

Table S2. Product formation of disulfide-containing prodrugs and ADC conjugates in incubation with TRX and GRX under various conditions

Reaction/ Condition	Cofactor	Parent→	3	5	10	12	13		
		Product→	1	1	1	2	2	16	11
+hTRX 2h	+NADPH		++	+	+	++	++	+	++
+hTRX 1h	+NADPH		ND	ND	ND	++	++	-	++
+rTRX 1h	+NADPH		ND	ND	ND	++	++	+	++
+hGRX 2h	+GSH		-	+	+	+	+	+	++
+hGRX 1h	+GSH		ND	ND	ND	+	-	+	+
+hGRX 2h	-GSH		ND	ND	ND	+	-	-	-
+hTRX+inhibitor 2h	+NADPH		ND	ND	ND	-	-	-	-
+hTRX 2h	-NADPH		-	-	-	-	-	-	-
-hTRX 2h	+NADPH		ND	ND	ND	-	-	-	-
-hGRX	+GSH		-	-	-	-	-	-	-

Note: ++, +, -, and ND shows decreasing amounts.

Figure 1S. Stability of disulfide-containing prodrugs in human and rat blood incubations

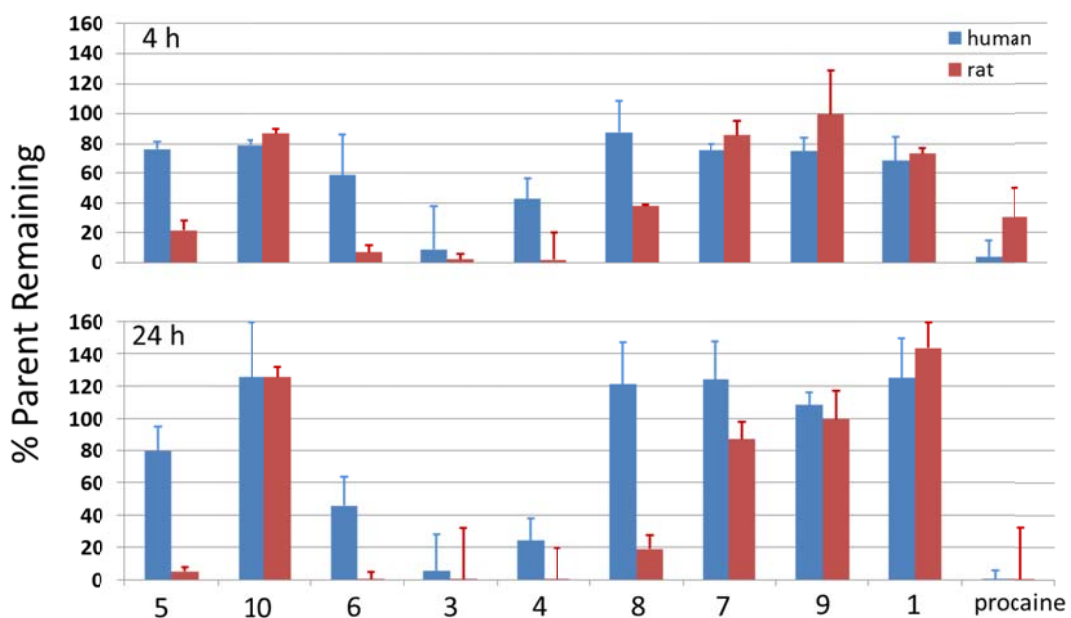
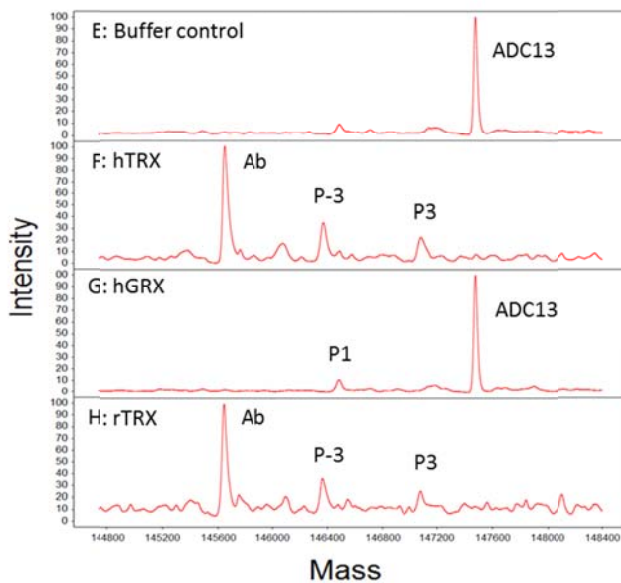
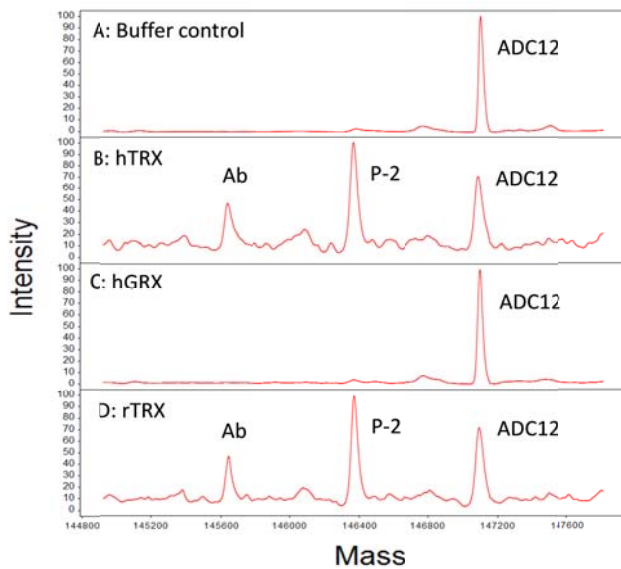


Figure 2S. Antibody-related product profiles of ADC **12** and **13** in incubations with TRX and GRX.

ADC12 = Ab + 2*LD; P-2 = Ab + LD

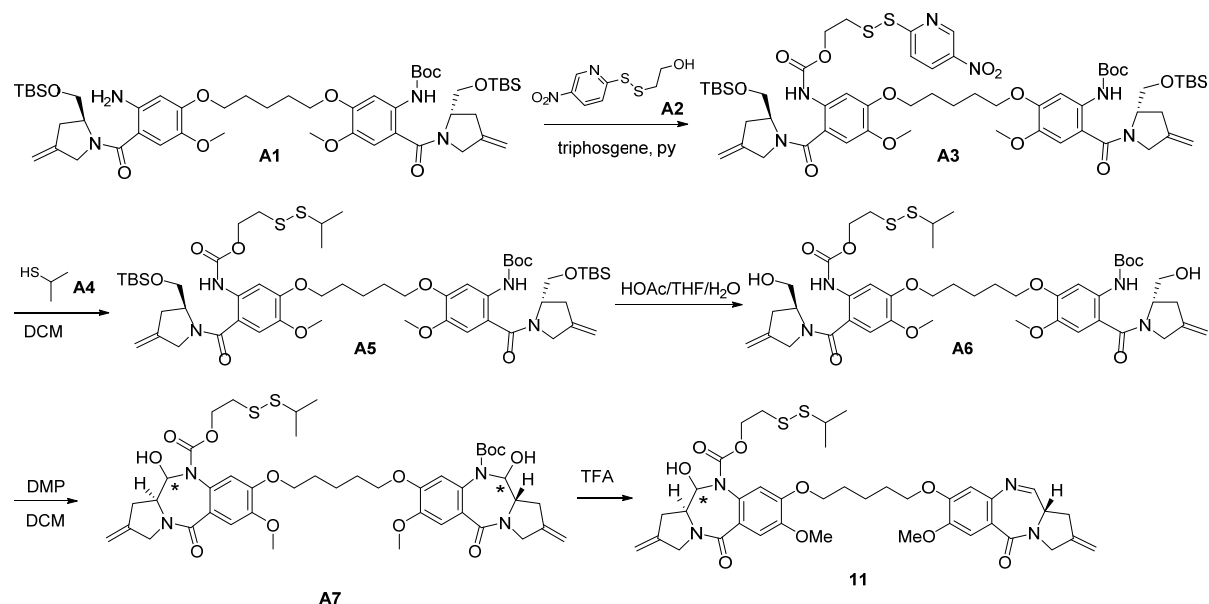
ADC13 = Ab + 2*LD; P-3=Ab+LD-196Da; P1=Ab+LD+CYS-196Da;

P3=Ab+2*LD-2*196Da; P4=Ab+2*LD-196Da



Synthesis of compounds

Compound 11



To a solution of triphosgene (89.43 mg, 0.300 mmol) and 4Å molecular sieves (50 mg) in DCM (5.0 mL) was added a solution of compound **A2** (165.0 mg, 0.710 mmol) and pyridine (168.58 mg, 2.13 mmol) in dichloromethane (DCM) (5.0 mL). The mixture was stirred at 0 °C for 30 min. The resulting mixture was added dropwise to a solution of compound **A1** (745 mg, 0.780 mmol), pyridine (169 mg, 2.13 mmol) and 4Å MS in DCM (5.0 mL). It was stirred at 0 °C for 30 min, and washed with water (5.0 mL). The organic phase was dried, concentrated and purified by flash column chromatography (5% MeOH in DCM) to give the product **A3** (698 mg, 81%) as a yellow oil. LC/MS (5-95, AB, 1.5 min): RT =1.187 min, m/z=606.5 [M/2+1]⁺.

To a solution of compound **A3** (698.0 mg, 0.580 mmol) in DCM (10.0 mL) was added 2-propanethiol (439 mg, 5.76 mmol). After the mixture was stirred at 20 °C for 1

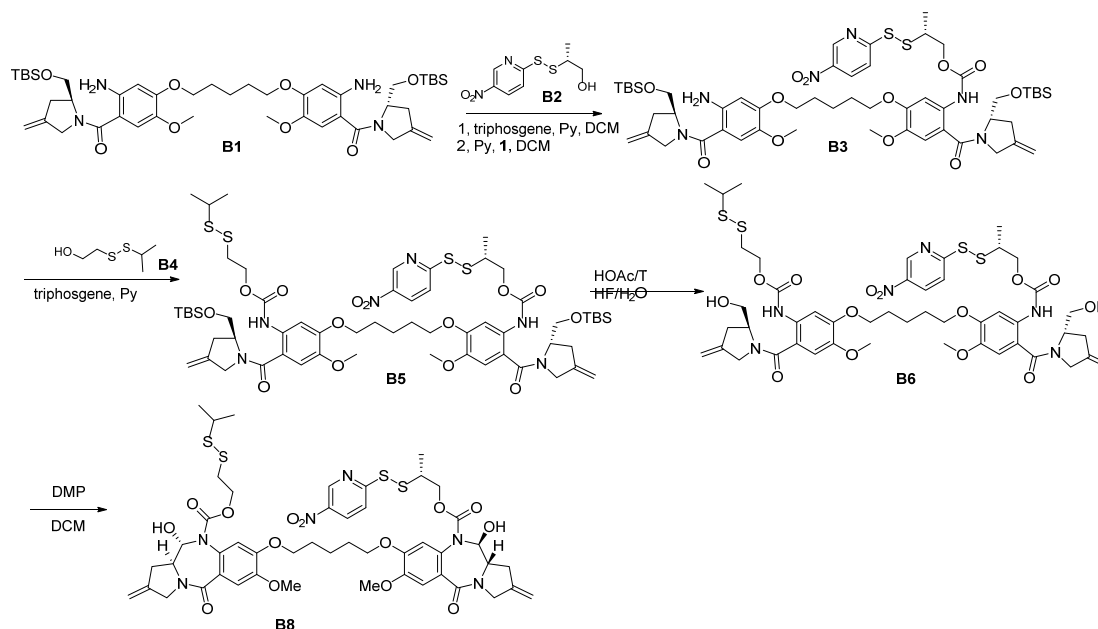
h, MnO_2 (100 mg) was added and stirred for 5 min, and filtered. The filtrate was concentrated and purified by prep-TLC (50% EtOAc in petroleum ether) to give compound **A5** (620 mg, 95%) as a yellow solid. LC/MS (5-95, AB, 1.5 min): RT = 1.221 min, m/z = 1131.4 $[\text{M}+1]^+$.

To a solution of compound **A5** (620.0 mg, 0.550 mmol) in THF (6.0 mL) and water (6.0 mL) was added HOAc (3.29 g, 54.8 mmol). The mixture was stirred at 40 °C for 16 h and concentrated. It was purified by column chromatography (10% MeOH in DCM) to afford compound **A6** (208 mg, 42%) as yellow oil. LCMS (5-95, AB, 1.5 min): RT = 0.854 min, m/z = 903.3 $[\text{M}+1]^+$.

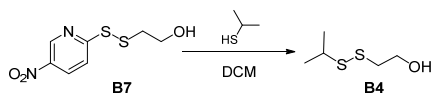
To a solution of compound **A6** (208.0 mg, 0.230 mmol) in DCM (8.0 mL) was added 4Å molecular sieves, DMP (224.7 mg, 0.530 mmol). The mixture was stirred at 20 °C for 2 h and was quenched with saturated NaHCO_3 and $\text{Na}_2\text{S}_2\text{O}_3$ solution (2.0 mL/2.0 mL). After it was stirred for 5 min, DCM (5.0 mL) was added and separated. The DCM phase was washed with water (2 x 5 mL). It was dried, concentrated and purified by prep-TLC (5% MeOH in DCM, R_f = 0.2) to afford compound **A7** (121 mg, 58%) as a light yellow foam. LC/MS (5-95, AB, 1.5 min): RT = 0.783 min, m/z = 781.3 $[\text{M}-100+1]^+$.

TFA (1.0 mL, 13.5 mmol) was added to compound **A7** (121.0 mg, 0.130 mmol) at 0 °C. After the mixture was stirred for 10 min, it was added to a cold saturated NaHCO_3 solution (20 mL) and extracted with DCM (3 x 10 mL). The combined organic layers were concentrated and purified by prep-TLC (10% MeOH in DCM, R_f = 0.2) followed by prep-HPLC (ACN, acetonitrile: 42~62%, 0.225%FA) to afford the title compound **11** (7.2 mg, 7.0%). LC/MS (5-95, AB, 1.5 min): RT = 0.868 min, m/z = 781.3 $[\text{M}+1]^+$.

Compound B8



Synthesis of INT4:



To a mixture of compound **B7** (200 mg, 0.86 mmol) in DCM (10 mL) was added 2-propanethiol (328 mg, 4.31 mmol). The mixture was stirred at 15 °C for 12 h. The solid was filtered and the solution was concentrated. The residue was purified by chromatography on silica (100% DCM) to give compound **B4** (90 mg, 69%) as a colorless oil. ¹HNMR (400 MHz, CDCl₃) δ 3.91-3.86 (m, 2 H), 3.05-3.00 (m, 1H), 2.86-2.84 (m, 2H), 2.04 (t, *J* = 6.4 Hz, 1H), 1.32 (d, *J* = 6.4 Hz, 1H).

To a solution of triphosgene (301 mg, 1.01 mmol) in DCM (5.0 mL) was added a mixture of compound **B2** (500 mg, 2.03 mmol) and pyridine (161 mg, 2.03 mmol) in DCM (5.0 mL) at 0 °C under N₂. The reaction mixture was stirred at 16 °C for 30 min. The mixture was concentrated in vacuo and used in the next step directly. To a solution

of the above mixture in DCM (5.0 mL) was added a mixture of compound **B1** (2.76 g, 3.24 mmol) and pyridine (128 mg, 1.62 mmol) in DCM (45.0 mL) at 0 °C. The reaction mixture was stirred at 0 °C for 1 h. TLC (50% EtOAc in petroleum ether R_f = 0.6) showed that the product **B3** was formed. The reaction mixture was concentrated in vacuo and purified by chromatography on silica (0-50% EtOAc in petroleum ether) to give compound **B3** (1.50 g, 78.2%) as a yellow solid. LC/MS (5-95, AB, 1.5 min): R_T = 1.09 min, m/z = 1126.7 $[M+1]^+$.

To a mixture of compound **B3** (200 mg, 0.18 mmol) and Et_3N (36 mg, 0.36 mmol) in DCM (4.0 mL) was added triphosgene (26 mg, 0.09 mmol) in DCM (2.0 mL) at 0 °C. After addition, the mixture was stirred at 15 °C for 20 min. LCMS (sample quenched with MeOH, 5-95, AB, 1.5 min): R_T = 1.164 min, m/z = 1183.4 $[M+32+1]^+$. The mixture was used directly in the next step. To above mixture was added a solution of compound **B4** (38 mg, 0.25 mmol) and Et_3N (34 mg, 0.33 mmol) in DCM (1.0 mL). After the reaction mixture was stirred at 15 °C for 2 h, it was concentrated and purified by prep-TLC (33% EtOAc in petroleum ether, R_f =0.4) to give compound **B5** (160 mg, 72%) as a yellow oil. LC/MS (5-95, AB, 1.5 min): R_T = 1.26 min, m/z = 1304.2 $[M+1]^+$.

To a mixture of compound **B5** (160 mg, 0.12 mmol) in THF (2.0 mL) and water (2.0 mL) was added HOAc (3.91 mL, 68 mmol) dropwise. After addition, the mixture was stirred at 15 °C for 12 h. TLC (5% MeOH in DCM, R_f = 0.5) showed was complete. The mixture was poured into EtOAc (30 mL), and was washed with water (10 mL x 2), saturated $NaHCO_3$ (10 mL x 2) and brine (10 mL). The organic layer was dried over Na_2SO_4 and purified by prep-TLC (5% MeOH in DCM, R_f = 0.5) to give compound **B6**

(120 mg, 93%) as a yellow solid. LC/MS (5-95, AB, 1.5 min): $R_T = 0.88$ min, $m/z = 1075.5$ $[M+1]^+$.

To a mixture of compound **B6** (60 mg, 0.06 mmol) in DCM (5.0 mL) was added DMP (71 mg, 0.17 mmol). The reaction mixture was stirred at 15 °C for 1 h. LCMS (5-95AB/1.5min): $R_T = 0.80$ min, $[M+H]^+ 1071.2$ showed 39% of desired product. The mixture was concentrated and the residue was purified by prep-TLC (7% MeOH in DCM, $R_f = 0.5$), followed by prep-HPLC (acetonitrile 45-75/10mM NH_4HCO_3 -ACN) to give **B8** (10.1 mg, 17%) as a white solid. LC/MS (5-95, AB, 1.5 min): $R_T = 0.81$ min, $m/z = 1053.1$ $[M-18+1]^+$. 1H NMR (400 MHz, $CDCl_3$) δ 9.22 (s, 1H), 8.30 (d, $J = 7.6$ Hz, 1H), 7.63 (d, $J = 8.8$ Hz, 1H), 7.27 (s, 1H), 7.21 (s, 1H), 6.86 (s, 1H), 6.70 (s, 1H), 5.59-5.56 (m, 2H), 5.15 (s, 4H), 4.43-4.29 (m, 4H), 4.17-3.64 (m, 19 H), 3.22-3.20 (m, 1H), 2.94-2.70 (m, 6H), 1.91 (d, $J = 6.4$ Hz, 4H), 1.64 (s, 2H), 1.26-1.20 (m, 9H).